Annals of Biology **42** (1) : 95-100, 2026 **http://agribioj.com** **Impact Score : 0.32 (Scopus)**

Fabrication and Characterization of TiO_2 - Nanoparticle Enhancing SPI Biocomposites for Food Packaging Applications

ANKUR KASHYAP, SWETA KUMARI, SANGITA YADAV, NISHA SETHI, NEHA LUHACH AND ASHA GUPTA*

Department of Environmental Science and Engineering, Guru Jambheshwar University of Science & Technology, Hisar-125 001 (Haryana), India
**(e-mail: gupta06amit@gmail.com; Mobile: 94163 72247)*

(Received: August 16, 2025; Accepted: October 7, 2025)

ABSTRACT

The current study focused on an integrative strategy using nanoparticles and soy protein to create a more advanced, sustainable and environmentally-friendly bio-based replacement to traditional plastic. The soy waste was used to isolate soy protein through a process that included pulverization, defatting, solubilization and centrifugation, followed by extraction, which was then combined with varying concentrations (0.25, 0.5 and 1%) of functionalized orange peel extract-based titanium dioxide nanoparticles. The produced 0.25, 0.5 and 1% nano-infused bioplastic sheets were subjected to various analytical tests employing techniques such as FTIR, SEM, DSC, water solubility, water transmission per cent (WVP), tensile strength and elongation to determine physiochemical and mechanical parameters. SEM and FTIR demonstrated substantial intermolecular interactions between SPI and nano-TiO_2. Pure SPI bioplastic sheets had the highest WVP (4.623±7.3 10-6.$gh^{-1}.m^{-1}.pa^{-1}$) and elongation at break (230%). While SPI/TiO_2 (w/w 1%) had a maximum Tensile Strength (TS) of 7 MPa. Thermal features enabled sustainability at temperatures of 134, 90.55, 91.17 and 96.22°C. Furthermore, a comparison was made between bare bioplastic sheets and nano-infused bioplastic sheets to distinguish the alterations that occured during the infusion of nanoparticles.

Key words: Soy protein isolate, nano-TiO_2, WVP, biodegradable composite film, elongation at break

INTRODUCTION

Petroleum-derived polymers are widely used due to their low density, economic viability, mechanical strength and ease of production in automotive parts, food packaging and others. However, their production uses limited fossil fuel resources, causing carbon dioxide emissions and toxic material releases (Yamada *et al*., 2020). Traditional plastics including polyethylene (PE), polypropylene (PP) and polyvinyl chloride (PVC) have little biodegradability and accumulate as rubbish in marine and terrestrial ecosystems for generations, according to Russo *et al*. (2019).

Bioplastics, particularly those made from renewable biomass, are a promising solution for environmental concerns. Bioplastics can be bio-based, biodegradable, or both (European Bioplastics, 2019). BIO-based and biodegradable plastics have garnered study attention due to their ability to reduce petroleum use and landfill waste. Various raw materials, including soy protein, cornhusk fibers and pig plasma protein, have been studied for bioplastic production via injection molding and extrusion (Álvarez-Castillo *et al*., 2021).

Due to availability, renewability and cost, soy protein is a popular bioplastic raw ingredient. The dry weight of soybeans has 40% protein, 20% lipids, 35% carbohydrates and 5% ash (Gamero *et al*., 2019). Soy flour (SF, 56%), soy meal (SM, 48%), soy protein isolate (SPI, 90%) and soy protein concentrate (SPC, 72%) have different protein contents depending on processing (Fernández Espada *et al*., 2016).

Soy protein's complex structure, primarily glycinin (11S) and â-conglycinin (7S), allows cross-linking via functional groups including SH, OH and NH residues (Gamero *et al*., 2019). Plasticizers or denaturing agents improve chain mobility and reduce intermolecular interactions in unmodified soy proteins (Fernández-Espada *et al*., 2016). Water and polyalcohols are common plasticizers, but glycerol is the most used since it lowers the glass transition temperature (Tg) and increases flexibility. Biodegradable polymers

from renewable resources are being studied as alternatives to petroleum-based plastics due to their environmental impacts. Soy protein-based bioplastics are versatile, cost-effective and compostable, making them appealing (Jiang *et al*., 2019). The lack of mechanical strength, moisture sensitivity and thermal stability often limits their practical applications. Integration of nanofillers, such as titanium dioxide (TiO_2) nanoparticles, has become a promising way to overcome these restrictions. TiO_2 nanoparticles enhance biopolymer matrices' effectiveness through reinforcing effects, UV resilience and antibacterial properties. Soy protein-based bioplastics using these nanoparticles improve mechanical properties, water absorption, and thermal stability. TiO, 's photocatalytic activity can help eliminate organic pollutants and promote self-cleaning, resulting in environmental benefits. Since literature is few, this integration strategy between metal oxide nanoparticles and soy-protein-based bioplastics to improve mechanical, thermal and barrier resistance needed further study.

This study investigated the formulation and characterization of bioplastics made from soy protein and TiO, nanoparticles. The study also analyzed the impact of nanoparticle concentration on the thermal, mechanical and barrier properties of bioplastics. This study investigated the biodegradability rate of bioplastics with increasing TiO, nanoparticle doses, aiming to provide sustainable, high-performance alternatives to traditional plastics.

MATERIALS AND METHODS

The process of extraction of soy protein isolate took place by using the aqueous extraction method (Nguyen *et al*., 2016; Preece *et al*., 2017; Luthria *et al*., 2018). In the method soy flour was defatted using n-hexane. Protein was isolated by solubilizing the defatted flour in alkaline water (pH 9.5), centrifuging, and precipitating the protein at its isoelectric point (pH 4.5) using HCl. TiO, nanoparticles were green-synthesized by adding an aqueous orange peel extract to titanium isopropoxide until a neutral pH was reached. The resulting precipitate was filtered, dried and calcined at 600 °C to obtain rutile TiO_2.

Bioplastic films were produced by dissolving SPI in water, adding glycerol as a plasticizer (50% w/w) and adjusting the pH to 8. Different concentrations of TiO, nanoparticles (0, 0.25, 0.5 and 1%) were incorporated into the cooled solution. The mixtures were cast onto plates and dried at 25±5°C for 48 h (Roufegarinejad, 2022).

The films were characterized using FTIR, which confirmed interactions between SPI and TiO_2. FE-SEM imaging showed surface morphology changes with nanoparticle addition. Thermal analysis (DSC) measured glass transition and melting temperatures. Mechanical testing revealed that tensile strength and strain at break were influenced by TiO, content.

Functional properties were also evaluated. The swelling ratio in water was calculated. Water vapor permeability (WVP) was measured using a standard cup method, where weight gain of a desiccant-filled cup sealed with the film was monitored over 24 h in a controlled environment (25°C, 50% RH).

The water solubility of the bioplastic was determined by its swelling ratio after 1 or 10 min in water, calculated using Equation 1:

$$\text{Swelling ratio (\%)} = 100\ (Ws / Wo)$$

Here, Wo and Ws were the initial and swollen weights, respectively (Jiménez-Rosado *et al*., 2021). Tensile strength was measured by applying axial force at 5 mm/min until fracture, assessing maximal stress and strain at break per a revised ISO 570-2:1993 standard. Water vapour permeability (WVP) was found using a modified cup method. A cup containing a desiccant was sealed with the film and placed at 25°C and 50% RH. The WVP was calculated based on weight gain over 24 h. All results were the average of five measurements.

$$WVTR = \frac{\Delta m}{\Delta t \times A} \quad ...(2)$$

$$WVP = \frac{WVTR \times FT}{\Delta p} \quad ...(3)$$

The WVP was calculated using equations 2 and 3, where WVTR and WVP denoted the water vapor transmission rate and water vapor permeability, A was the exposed surface area

of bioplastic film, $\Delta m/\Delta t$ represented the rate of water gain, FT showed thickness of the film and lastly Δp was showing the difference between partial water vapour pressure across the film. All measurements were performed in three replicates to ensure statistical reliability (Han *et al*., 2018; Vyas *et al*., 2025).

RESULTS AND DISCUSSION

Fig. 1. represents the FESEM images of the samples. Their unmodified soy based bioplasticin (Fig. 1a) displayed a rough surface with fissures. However, a visible alteration was seen in the surface texture from rough to smooth with increasing % of titanium dioxide nanoparticles. Morever, bubble formation in the form of microstructures was present in 0.25% TiO_2 infused SPI sheet (Fig. 1b). Beside these agglomeration, when the concentration of TiO_2 nanoparticle shift from 0.25% to 1%, these microstructures got erased as shown in Fig. 1d. The possible reason behind the absence of microstructure was the robust interaction which occured between molecules of soy protein isolate and molecules of TiO_2 that resulted in a stronger, smoother and compact structure of bioplastic sheet. Consequently, Fig. 1c representing 0.5% TiO_2 infused SPI sheet, exhibited the least agglomeration to contrast to the bare and 0.1% sheets. Salarbashi *et al*. (2018), Roufergarinejad (2022) and Hu *et al*. (2023) demonstrated analogous findings.

IR radiation transmission differences due to functional group vibrational modes caused major and minor FTIR peaks. Materials vary in raw composition and synthesis method, affected functional groups and vibrational modes. The FTIR spectra of SPI and TiO2 nanoparticle-based bioplastic sheets showed dominant peaks around wave numbers 3400/cm, 2960/cm, 1639/cm, 1384/cm and 600/cm, which correspond to O-H/N-H, -CH2, C=O, C-N, C-C, and Ti-O-Ti bonds stretching and vibration (Fig. 2) with increasing nanoparticle percentage, SPI-TiO2 bioplastic sheet peak shifting was also observed. SPI spectral peak at 3414/cm broadens to 3427/cm in 1% TiO2 infused SPI sheet. This peak in SPI sheets was due to amide N-H stretching and hydrogen bonding, while in nanopartiocle infused sheets it was due to water molecule O-H bond vibrations. The peaks at 1639/cm and 1533/cm corresponded to C=O and C-N stretching related to amide III group (Roufegarinejad,

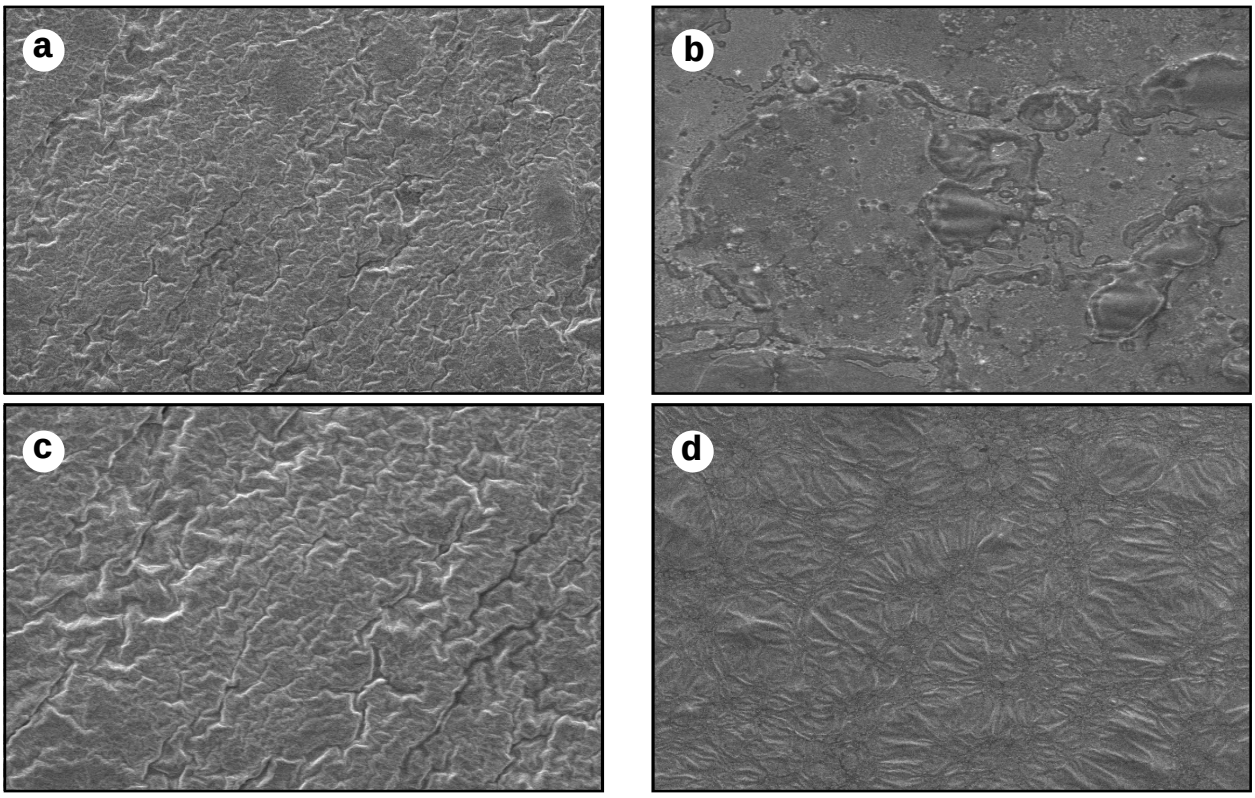

Fig. 1. SEM images of (a) Soy-based bioplastic, (b) SPI/TiO_2 0.25%, (c) SPI/TiO_2 0.50% and (d) SPI/TiO_2 1%.

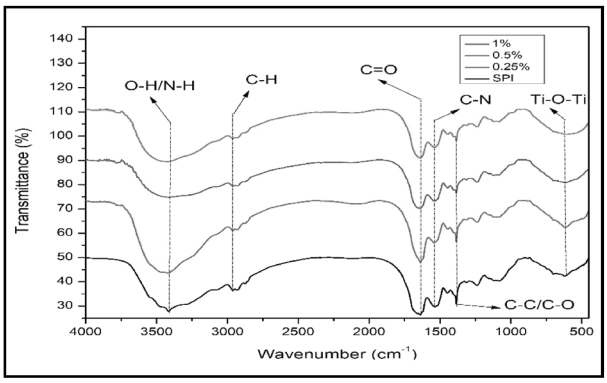

Fig. 2. FTIR spectra of SPI sheets and SPI/TiO_2 different concentration sheets.

2022), while the peak at 2960/cm and 1384/cm showed assymetrical -CH2 group stretching and C-O bond stretching of glycerol molecules in SPI spectrum (Sharma *et al*., 2023).

SPI had the highest water solubility of all evaluated films (Fig. 3). Metal oxide nanoparticles (NPs) as nanofillers created a convoluted channel that prevented water molecules from diffusing across the film matrix, increasing its water resistance. Table 1 represents SPI film and TiO_2 infused films along with their calculated water solubility following a descending order of SPI film (70%) > SPI/TiO_2-0.25 (62%) > SPI/TiO_2-0.50 (53%) > SPI/TiO_2-1 (43.4%). Heat treatment during film preparation caused protein molecules to establish strong intermolecular contacts, particularly disulfide bonds, which caused partial insolubility. By occupying interstitial spaces between polymer chains, uniform NP dispersion in the polymer matrix compacted and densified the structure, limiting water penetration.

FTIR spectroscopy indicated that hydrogen bonding between the SPI matrix and NPs limited film hydrophilic group availability. SPI-

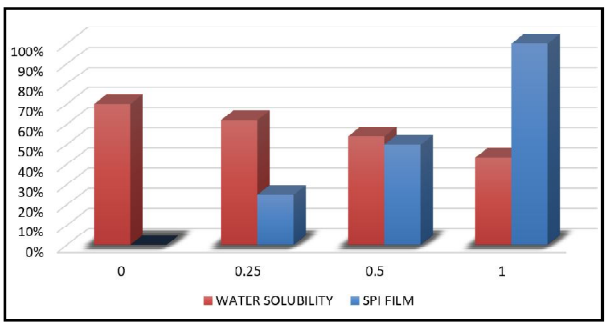

Fig. 3. Relation between water solubility w.r.t. nanoparticle concentrations.

Table 1. Water solubility of film

Film	Water solubility (%)
SPI Film	70
SPI/TiO_2 (0.25%)	62
SPI/TiO_2 (0.50%)	54
SPI/TiO_2 (1%)	43.4

based nanocomposite films' water resistance improved due to these factors.

The films' mechanical properties were tested by uniaxial tensile strength. Stress-strain curves during testing indicated bioplastic film tensile strength (TS) and elongation at break (%E). The tensile test film's maximum stress was TS. Fig. 4 and 5 show that soy-based bioplastic with higher nanoparticle concentration had higher tensile strength. In contrast, bioplastic elongation upon break implied flexibility. Tensile strength and elongation at break were inversely related. Elongation decreased with TiO_2 nanoparticle concentration, yet the naked soy bioplastic had the highest EB, while the improved formulation with 0.50 SPI/TiO_2 had the greatest stretchability. Numerous studies showed that protein-based films were flexible but weak; nanoparticles increased their tensile strength (Roufegarinejad, 2022; Yao *et al*., 2025).

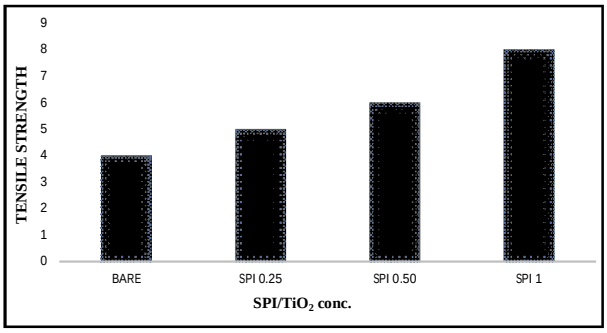

Fig. 4. Tensile strength vs. nanoparticle concentration.

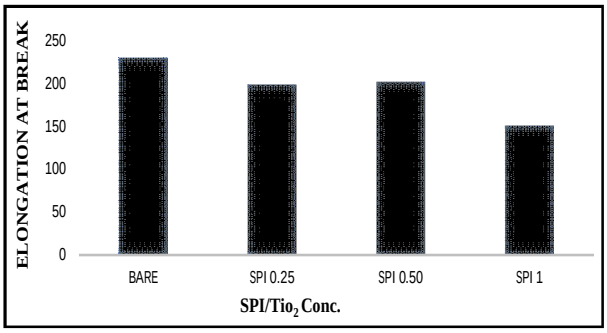

Fig. 5. Elongation at break vs. nanoparticle concentration.

Fig. 6 shows the thermal behaviour of SPI and SPI+TiO2 at 0.25, 0.50 and 1%. The DSC analysis found that the glass transition temperature (Tg) of bioplastics was 134, 90.55, 91.17 and 96.22°C. Proteins changed from glassy to rubbery at Tg. The pure sample had a high enthalpy (102.46 J/g), indicating a phase transition (crystalline melting). Soy-based samples had modest enthalpy values (0.3-0.4 J/g), suggesting weak thermal events due to their amorphous nature (0.05% soy/titanium dioxide). Soy samples with the highest enthalpy (0.411 J/g) showed little aggregation. 1% Soy/TiO2 had the lowest enthalpy (0.287 J/g), probably due to homogeneity or insufficient reinforcing phases. 0.25% Soy/TiO2: intermediate enthalpy (0.339 J/g), peak temperature slightly below 0.05. Soy addition to bioplastic decreased thermal stability but improved biodegradability (Jiménez-Rosado *et al*., 2021).

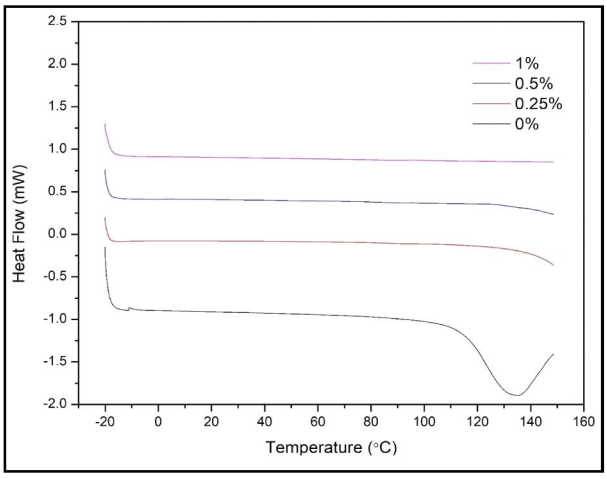

Fig. 6. DSC plot of bioplstic samples showing temperature vs. heat flow rate.

In the research field on packaging materials, Water Vapour Permeability is very essential due to its hydrophobicity that protects the material from environmental factors. WVP is influenced by factors such as film thickness, porosity, hydophilicity, porebending and hydophilicity. Nanoparticles incorporation decreased the WVP by creating resistance towards the moisture with compromising its actual properties. Table 2 shows the decreased value of SPI/TiO_2 (1%) was 3.14 $gm^{-1}.day^{-1}.pa^{-1}$. With incorporation of NPs WVP gradually decreased.

The degradation rate of the soil burial test was calculated from weight loss over time. The

Table 2. Representation of WVP values of nano-infused bioplastics

Film	WVP ($10^{-6}.gh^{-1}.m^{-1}.pa^{-1}$)
Bare	4.623±0.73
0.25% SPI/TiO_2	3.868431128±0.86
0.50% SPI/TiO_2	3.84709274±1.1
1% SPI/TiO_2	3.14182994±2.6

European standard EN13432 (Amin *et al*., 2019) informed that biodegradable plastics had 90% of their mass fragmented in water, CO_2 and biomass in six months. Fig. 7 shows the degradation setup of bioplastics under laboratory conditions. After 10 days of burial in moist soil under laboratory conditions, bare SPI/TiO_2 showed 80% degradation due to microbial attack on soy protein peptide chains. In contrast, the composites degraded more slowly: 0.25% SPI/TiO_2 degraded by 60%, 0.50% SPI/TiO_2 by 68.75% and 1% SPI/TiO, by 54.75% (Das *et al*., 2025).

Fig. 7. Degradation of bioplastic under laboratory conditions.

CONCLUSION

This work analyzed SPI-based films with varying concentrations of nano-TiO_2 for their physico-chemical and structural properties. Results showed that SPI/TiO_2 film exhibited the maximum tensile strength of nearly 7 Mpa which was better than as compared to others. WVP properties showed the comparable values between SPI/TiO_2 0.25% and 0.5% with 3.86 and $3.8410^{-6}.gh^{-1}.m^{-1}.pa^{-1}$ While the least value showed by 1% composite that made it more efficient for packaging. Thermal properties also showed good thermal properties of sheets. Subsequent analysis of degradation indicated that bare samples exhibited greater degradation compared to others, while the 1% composite demonstrated the least degradation. Therefore, one can say that nanoparticles addition in soy based bioplastics improved its

properties. Additional research is necessary to enhance its hydrophobic properties. Different nanomaterials can be used to further enhance its properties for making it more efficient in packaging applications.

REFERENCES

Álvarez-Castillo, E., Bengoechea, C. and Guerrero, A. (2021). Strengthening of porcine plasma protein superabsorbent materials through a solubilization freeze drying process. *Polymers* **13**: 772. *doi:10.3390/polym 13050772.*

Amin, M. R., Chowdhury, M. A. and Kowser, M. A. (2019). Characterization and performance analysis of composite bioplastics synthesized using titanium dioxide nanoparticles with corn starch. *Heliyon* **5**: 2009. *doi:10.1016/j.heliyon.2019.e02009.*

Das, R., Singh, R., Pooja, L. R., Darjee, S., Vashisth, A., Kumar, T. A. and Shrivastava, M. (2025). Corn cob-derived bioplastics infused with titanium dioxide nanoparticles: Synthesis and functional assessment. *Waste Biomass Val*. **16**: 3773-3787. *doi:10.1007/s12649-025-02907-y.*

Fernández Espada, L., Bengoechea, C., Cordobés, F. and Guerrero, A. (2016). Protein/glycerol blends and injection-molded bioplastic matrices: Soybean versus egg albumen. *J. Appl. Polymer Sci.* **133**: *doi:10.1002/ app.42980.*

Gamero, S., Jiménez-Rosado, M., Romero, A., Bengoechea, C. and Guerrero, A. (2019). Reinforcement of soy protein-based bioplastics through addition of lignocellulose and injection molding processing conditions. *J. Polym. Environ*. **27**: 1285-1293.

Han, Y., Yu, M. and Wang, L. (2018). Physical and antimicrobial properties of sodium alginate/carboxymethyl cellulose films incorporated with cinnamon essential oil. *Food Pack. Shelf Life* **15**: 35-42. *doi: 10.1016/j.fpsl.2017.11.001.*

Hu, J., Li, D., Huai, Q., Geng, M., Sun, Z., Wang, M. and Zheng, H. (2023). Development and evaluation of soybean protein isolate based antibacterial nanocomposite films containing nano-TiO_2. *Indust. Crops Prod*. **197**: 116620. *doi:10.1016/j.indcrop. 2023.116620.*

Jiang, L., Liu, Y., Li, L., Qi, B., Ju, M., Xu, Y. and Sui, X. (2019). Covalent conjugates of anthocyanins to soy protein: Unravelling their structure features and *in vitro* gastrointestinal digestion fate. *Food Res. Int*. **120**: 603-609. *doi:10.1016/j.foodres. 2018.11.011.*

Jiménez-Rosado, M., Perez-Puyana, V., Sánchez-Cid, P., Guerrero, A. and Romero, A. (2021). Incorporation of ZnO nanoparticles into soy protein-based bioplastics to improve their functional properties. *Polymers* **13**: **486**. *doi:10.3390/polym13040486.*

Luthria, D. L., Maria John, K. M., Marupaka, R. and Natarajan, S. (2018). Recent update on methodologies for extraction and analysis of soybean seed proteins. *J. Sci. Food and Agric.* **98**: 5572-5580.

Nguyen, Q., Hettiarachchy, N., Rayaprolu, S., Jayanthi, S., Thallapuranam, S. and Chen, P. (2016). Physico-chemical properties and ACE-I inhibitory activity of protein hydrolysates from a non-genetically modified soy cultivar. *J. Am. Oil Chem. Soc.* **93**: 595-606. *doi:10.1007/s11746-016-2801-1.*

Preece, K. E., Hooshyar, N. and Zuidam, N. J. (2017). Whole soybean protein extraction processes: A review. *Innovative Food Sci. & Emerging Technologies,* **43**: 163-172.

Roufegarinejad, L. (2022). Development and characterization of the reinforced soy protein isolate-based nanocomposite film with CuO and TiO_2 nanoparticles. *J. Poly. Environ*. **30**: 2507-2515.

Russo, I., Confente, I., Scarpi, D. and Hazen, B. T. (2019). From trash to treasure: The impact of consumer perception of bio-waste products in closed-loop supply chains. *J. Cleaner Prod*. **218**: 966-974.

Salarbashi, D., Tafaghodi, M. and Bazzaz, B. S. F. (2018). Soluble soybean polysaccharide/ TiO_2 bionanocomposite film for food application. *Carb. Poly*. **186**: 384-393.

Vyas, A., Ng, S. P., Fu, T. and Anum, I. (2025). ZnO-embedded carboxymethyl cellulose bioplastic film synthesized from sugarcane bagasse for packaging applications. *Polymers* **17**: 579. *doi:10.3390/polym 17050579.*

Yamada, M., Morimitsu, S., Hosono, E. and Yamada, T. (2020). Preparation of bioplastic using soy protein. *Int. J. Biol. Macro.* **149**: 1077-1083.

Yao, L., Sun, H., Yu, C. and Weng, Y. (2025). Enhanced xylan/PVA composite films via nano-zno reinforcement for sustainable food packaging. *Polymers* **17**: 1080. *doi: 10.3390/polym17081080.*